Published in final edited form as:
Bone. 2011 February 1; 48(2): 275–280. doi:10.1016/j.bone.2010.09.028.

Disruption of bone development and homeostasis by trisomy in Ts65Dn Down syndrome mice

Joshua D. Blazek[a], **Anna Gaddy**[a], **Rachel Meyer**[a], **Randall J. Roper**[a,b], and **Jiliang Li**[a]

[a]Department of Biology, Indiana University-Purdue University Indianapolis and Indiana University Center for Regenerative Biology and Medicine, 723 W. Michigan Street, SL306, Indianapolis, IN 46202, USA

Abstract

Down syndrome (DS) is a genetic disorder resulting from trisomy 21 that causes cognitive impairment, low muscle tone and craniofacial alterations. Morphometric studies of the craniofacial and appendicular skeleton in individuals with DS suggest that bone development and homeostasis are affected by trisomy. The Ts65Dn mouse model has three copies of approximately half the genes found on human chromosome 21 and exhibits craniofacial skeletal and size differences similar to those observed in humans with DS. We hypothesized that Ts65Dn and euploid mice have distinct differences in bone development and homeostasis influencing both the craniofacial and appendicular skeletal phenotypes. Quantitative assessment of structural and mechanical properties of the femur in Ts65Dn and control mice at 6 and 16 weeks of age revealed significant deficiencies in trabecular and cortical bone architecture, bone mineral density, bone formation, and bone strength in trisomic bone. Furthermore, bone mineral density and dynamic dentin formation rate of the skull and incisor, respectively, were also reduced in Ts65Dn mice, demonstrating that trisomy significantly affects both the craniofacial and appendicular skeleton.

Keywords

Trisomy; Down syndrome; mouse models; bone homeostasis; genetics

Introduction

Down syndrome (DS) is caused by the triplication of human chromosome 21 resulting in genetic dosage imbalance thought to affect several different developmental pathways. DS occurs in 1 in 700-800 live births [1], and there are approximately 80 clinically defined phenotypes associated with DS, including defects in the central nervous, cardiac, and skeletal systems [2-5]. Craniofacial abnormalities are common to all individuals with DS and include microcephaly, small maxilla and mandible, reduced midface, and brachycephaly [6]. Individuals with DS also exhibit alterations in the size of the cranial base, including shorter and flatter anterior and posterior bases [7]. In addition to craniofacial skeletal abnormalities, it has been suggested that individuals with DS exhibit alterations in the development and maintenance of their appendicular skeletons [8].

[b]Corresponding Author: Randall J. Roper, Ph.D., Department of Biology, Indiana University-Purdue University Indianapolis, 723 W. Michigan Street SL 306, Indianapolis, IN 46202, Phone: (317) 274-8131, Fax: (317) 274-2846, rjroper@iupui.edu.

The establishment of the appendicular skeleton begins early in prenatal development and continues through adolescence, and previous studies in humans have shown that individuals with trisomy have altered bone development both pre- and postnatally [8,9]. Prenatal evidence suggesting changes in DS bone development has been derived from ultrasound measurements of the long bones [10]. During the second trimester, humerus and femur lengths are shorter, on average, in fetuses with DS and these measurements are used as a predictor for trisomy 21 [11,12]. Postnatally, individuals with DS may exhibit severe reductions in stature resulting from alterations in the normal pattern of skeletal growth [8]. Furthermore, studies have suggested the mineral properties of bone are altered in individuals with DS. Individuals with DS exhibit a reduction in areal bone mineral density (BMD) in the spine, hip, and total body [13], as well as strength in the femoral neck [14]. Despite a gross structural understanding of the cranial and appendicular skeletal phenotypes, little is known about the origin and consequences of altered bone development in individuals with DS.

The use of mouse models to study human conditions provides a controlled environment and the tissue necessary to extensively study bone phenotypes associated with trisomy. The Ts(17^{16})65Dn mouse (Ts65Dn), the most widely used model in the study of DS, has a small translocation chromosome that results in the triplication of approximately half the gene orthologs found on human chromosome 21 [15-17]. Ts65Dn mice exhibit numerous phenotypes parallel to those observed in humans including cognitive impairment, neurological structural deformities, craniofacial defects, and cardiovascular anomalies [18-20]. Specifically, Ts65Dn mice have several characteristic DS craniofacial defects including a shortened rostrum, smaller neurocranium along the rostro-caudal axis, reduced ossification in the frontal and parietal bones at birth, and reduced mandible size [6,21]. In addition to having similar phenotypes to humans with DS, the predictive nature of Ts65Dn mouse phenotypes, as demonstrated in the cerebellum, suggests it is a powerful model to study the impact of trisomy on bone development and homeostasis [22].

We hypothesized that Ts65Dn as compared to euploid mice exhibit altered bone development and homeostasis in the skeleton of growing and adult mice. We examined femurs, skulls, and mandibles from 35 euploid and 39 trisomic 6 and 16 week old mice. Femurs were subjected to microCT (μCT) imaging, DXA bone densitometry scanning, and mechanical testing to elucidate the physical and mechanical properties of the bone. Femurs and mandibles were sectioned and analyzed to determine bone formation rates. We report that the physical and mechanical properties of bone are significantly altered in Ts65Dn mice.

Materials and Methods

Animals

Female B6EiC3Sn a/A-Ts(17^{16})65Dn (Ts65Dn) and female and B6.129S4-Gt(ROSA)26Sor^{tm1Sor}/J (B6.R26R) and C3H/HeJ (C3H) mice were purchased from the Jackson Laboratory (Bar Harbor, ME). B6(R26R)C3F$_1$ mice were bred by crossing B6.R26R females with C3H males. Ts65Dn males were generated at Indiana University-Purdue University Indianapolis (IUPUI) by crossing Ts65Dn females with B6(R26R)C3F$_1$ males and identified by FISH genotyping {Moore, 1999 #^{43}}. Ts65Dn (approximate 50% B6 and 50% C3H background with small marker (trisomic) chromosome) mothers generated the 39 trisomic and 35 euploid male mice used for this study. Only male mice were used due to the subfertile nature of Ts65Dn male mice and importance of Ts65Dn female mice in colony maintenance. Trisomic and euploid mice were split into two groups and allowed to age to either 6 (Eu, n= 17; Ts, n= 17) or 16 (Eu, n= 18; Ts, n= 22) weeks. At these respective time points, mice were sedated using a 1:1 solution of isofluorane and mineral oil and injected intraperitoneally with 0.2ml of 0.6% Calcein green dye diluted in saline

solution, as well as four days later with 0.2 ml of 1.0% Alizarin red dye. Three days after the Alizarin red injection mice were sacrificed and weighed. The femur, mandible, and skull were subsequently extracted. The right femur and skull were wrapped in gauze soaked in saline solution and the mandible was placed in 70% ethanol. Femurs and skulls were frozen and stored at -20°C until further use and the mandibles were kept at room temperature. All animal use and protocols were approved by the School of Science IACUC committee at IUPUI.

Dual Energy X-ray Absorptiometry (DXA)

The bone mineral content of the femurs and skulls was analyzed using the Lunar Piximus DXA machine (PIXImus Lunar Corp., Madison, WI). The machine was calibrated prior to each use. The femurs and entire skulls were placed caudal side down on the densitometer and scanned using ultrahigh resolution (0.18 mm × 0.18 mm) [23]. Lunar Piximus 2 2.0 software was used to assess BMD, bone mineral content (BMC), and total bone area.

MicroCT imaging and Analysis

Femurs were imaged using the SkyScan 1172 microCT (SkyScan, Kontich, Belgium). Femurs were thawed in 0.9% saline, wrapped in parafilm, and placed in a styrofoam mold fitted to the rotating stage in the machine. The scanning parameters were set as follows: voltage 60kV, resolution 6μm, binning mode 2k, and filter Al 0.5mm. A reconstruction and analysis was conducted on each set of images using CTrecon and CTan software from Skyscan with the following parameters: post alignment variable, smoothing 2, ring artifact reduction 5, beam hardening 20, and threshold 0-0.11. A region of interest was created composing of the boundaries of trabecular bone in the distal femur and 1mm of tissue, proximal to the growth plate was analyzed. 3D analysis was conducted on the trabecular bone to obtain the percent bone volume and trabecular number, thickness, and separation measurements. For cortical bone analysis the bone at the midshaft of the femur was traced and 2D analysis was conducted on a single section to obtain the total and bone areas, periosteal perimeter, and mean polar moment of inertia (MPMI) (calculated from CTan). The anterior-posterior diameter and average cortical thickness of a femur midshaft cross-section was measured using CTan to calculate the cross-sectional moment of inertia (CSMI; $CSMI = \pi * [(AP\ diameter - cortical\ thickness)^3 * cortical\ thickness]/8$) [24]. Variation for the microtomographic measurements used in this study has been shown to be very reproducible and reveal the precision of the instruments used [27,28].

Tissue Processing and Histomorphometry

The left femur and mandible were dehydrated in graded levels of ethanol, cleared in xylene, and embedded in methyl methacrylate. A diamond-embedded wire-saw (Histo-saw; Delaware Diamond Knives, Wilmington, DE) was used to cut transverse thick sections of the mandible and femur (400 μm and 200 μm, respectively). The femurs were further ground down to 30 μm, and then mounted unstained to microscope slides using Eukitt [23], to enhance the viewing of the fluorescent label. Mandibles were not ground because it was deemed unnecessary as clear images were obtained of the original sections. One section per mandible and femur was read using a D-FL Epi-Fluorescence attachment on a Nikon Eclipse 80i DIC microscope, and images were taken using a Nikon DS-Fi1 digital sight camera. Mineralizing surface/bone surface (MS/BS) was assessed by measuring the double label surface (dL.S), single label surface (sL.S), and total surface (BS) using BioQuant software (R & M Biometrics, Nashville, TN; MS/BS = (dL.S.+ 0.5*sL.S)/BS). Mineral apposition rate (MAR) was determined by measuring the average distance between the two fluorochrome labels, using Image J (National Institute of Health, Bethesda, MD), and dividing the distance by the 4 days between label administration. MS/BS and MAR were used to calculate bone formation rate (BFR; BFR=MS/BS*MAR*365 days; μm3/μm2/year).

Dynamic measures of bone formation were made at the periosteal surface of the femur midshaft and the inner surface of the developing incisor.

Mechanical Testing

The strength of the femur was determined by 3-point bending [25] using a miniature materials machine. The femurs were thawed slowly at room temperature, and then placed posterior side down on the 3-point bending apparatus with lower supports fixed at a distance of 7 mm apart and held constant for all of the femurs tested. The femur was positioned in a manner so that the force would be applied to the midpoint of the bone. The femur was preloaded using 0.1N to establish contact with the bone. The displacement rate was set at 0.1 mm/sec. Once preloaded, force was applied until the bone was broken. Data was gathered by the system and Microsoft Excel was used to determine the ultimate load, energy to failure, and stiffness of the bone. Furthermore, the material properties of the femur were calculated by normalizing the structural parameters as previously described [26]. Briefly, the material level properties were calculated as follows:

$$\text{Ultimate stress} = (\text{ultimate load} * L * \text{APdia})/(8 * \text{CSMI})$$

$$\text{Modulus} = (\text{stiffness} * L^3) / (48 * \text{CSMI})$$

$$\text{Toughness} = (0.75 * \text{energy absorption} * \text{APdia}^2) / (L * \text{CSMI})$$

where L represents the span between the bottom supports, and APdia and CSMI were from microCT images.

Statistical Analysis

Data were analyzed using a standard 2-tailed t-test and significance was denoted by p-values less than or equal to 0.05.

Results

Segmental trisomy effects bone mineral composition in the Ts65Dn femur and skull

To compare the density of the individual bones between Ts65Dn and euploid mice, femurs and skulls were analyzed using DXA. Ts65Dn mice had significantly less bone area in both the femur and skull at 6 and 16 weeks when compared to euploid littermates (Table 1). In addition to bone area, Ts65Dn mice exhibit significantly lower BMD and BMC at both time points in the femur and skull compared with euploid littermates (Table 1). This suggests that both size and density of bone in the appendicular and axial skeleton are affected by segmental trisomy in the Ts65Dn mouse.

The microstructure of the femur is altered in Ts65Dn mice

To understand differences in the microstructure of the generalized skeleton ofTs65Dn and euploid mice, microCT imaging was performed on the distal end (trabecular bone) and midshaft (cortical bone) of 6 and 16 week old (Figure 1A; Figure 2A, respectively) Ts65Dn and euploid femurs. Ts65Dn mice exhibited a significantly lower BV/TV (Figure 1B) at 6 (12.88% ± 1.92 SEM) and 16 weeks (16.16% ± 1.13) of age when compared to euploid littermates (22.51% ± 1.90; 21.51% ± 1.88, respectively). To determine changes in structural properties, trabecular number, separation, and thickness were assessed. At both time points Ts65Dn mice exhibited significantly lower trabecular number (6 wks, Eu, 4.01 mm^{-1} ± 0.26; Ts, 2.46 mm^{-1} ± 0.31; 16 wks, Eu, 3.69 mm^{-1} ± 0.28; Ts, 2.89 mm^{-1} ± 0.22; Figure 1C), and significantly higher trabecular separation (6 wks, Eu, 0.15 mm ± 0.01; Ts, 0.21 mm ± 0.02; 16 wks, Eu, 0.18 mm ± 0.01; Ts, 0.21 mm ± 0.01; Figure 1D). Trabecular thickness (Figure

1E) was lower in Ts65Dn mice, but the difference was not significant at either time point (6 wks, p= 0.07; 16 wks, p= 0.19).

Cortical bone analysis of the Ts65Dn and euploid femoral midshaft in 6 and 16 week old mice (Figure 2A) showed significantly lower mean total cross-sectional area (6 wks, Eu, 0.89 mm ± 0.04,; Ts, 0.71 mm ± 0.04; 16 wks, Eu, 1.13 mm ± 0.03; Ts, 0.99 mm ± 0.04; Figure 2B) and mean total periosteal perimeter (6 wks, Eu, 9.78 mm ± 0.12; Ts, 8.68 mm ± 0.21; 16 wks, Eu, 10.62 mm ± 0.28; Ts, 9.98 mm ± 0.23) in Ts65Dn mice when compared to euploid littermates. Furthermore, mean polar moment of inertia (MPMI), an estimate of the ability of an object to resist bending, was also significantly lower in Ts65Dn mice as compared to euploid littermates (6wks, Eu, 0.46 mm ± 0.02; Ts, 0.28 mm ± 0.03; 16 wks, Eu, 0.63 mm ± 0.04; Ts, 0.51 mm ± 0.03). Overall, the combination of trabecular and cortical structural phenotypes in the Ts65Dn mouse femur suggest a severe reduction in the size and strength of the trisomic long bone.

The rate of mineralization is reduced in the Ts65Dn mouse model

Alterations in BMD and the bone microstructure at 6 weeks of age suggested possible deficiencies in bone accrual. We assessed dynamic bone formation properties via fluorescent analysis using two labels (Calcein green and Alizarin red), injected 4 days apart, in cross-sections of the incisor and femur (Figure 3A). Ts65Dn and euploid mice had a similar mineralizing surface (MS/BS), an estimate of active osteoblast number, in the incisors (Eu, 0.86 ± 0.02; Ts, 0.81 ± 0.03) and femurs (Eu, 0.76 ± 0.04; Ts, 0.71 ± 0.05) at 6 weeks of age (Figure 3B). Despite an estimated similar number of active osteoblasts, Ts65Dn mice exhibited a significantly lower mineral apposition rate (MAR; Figure 3C) on the periosteal surface of the femur (Eu, 2.39 μm/day ± 0.21; Ts, 1.61 μm/day ± 0.15) and incisor (Eu, 3.79 μm/day ± 0.17; Ts, 2.77 μm/day ± 0.23) in 6 week old Ts65Dn mice. Bone and dentin formation rates (BFR, DFR; Figure 3D) were also found to be significantly lower in the femur (Eu, 629.55 ± 49.49; Ts, 411.56 ± 34.10) and incisor (Eu, 1195.53 ± 76.50; Ts 827.19 ± 100.13), respectively, in Ts65Dn mice. These data indicate the formation rate of new cortical bone (femur) and dentin (incisor) is severely affected by segmental trisomy.

Reduced strength in the femur of Ts65Dn mice

To determine if the documented physical and chemical changes affected the structural and material properties of the Ts65Dn femur, we conducted 3-point bending on the femur at 6 and 16 weeks of age in Ts65Dn and euploid mice. Structurally, the Ts65Dn femur had a significantly lower ultimate load (6 wks, Eu, 22.51 N ± 3.70; Ts 16.36 N ± 1.21; 16 wks, Eu, 24.98 N ± 1.29; Ts, 21.47 N ± 0.88; Table 2) compared with euploid mice. Similarly, the Ts65Dn femur exhibited lower stiffness (6 wks, Eu, 11.15 N/mm ±2.67; Ts, 6.91 N/mm ± 0.63; 16 wks, Eu, 29.67 N/mm ± 2.34; Ts, 24.40 N/mm ± 0.89; Table 2) and energy to failure (6 wks, Eu, 5.73 N*mm ± 1.23; Ts, 4.08 N*mm ± 0.31; 16 wks, Eu, 11.86 N*mm ± 0.53; Ts, 10.24 N*mm ± 0.60; Table 2) at both time points, although the difference in energy to failure at 16 weeks of age was nearing statistical significance (p= 0.06). At the material level, we found no significant differences in ultimate stress or modulus. Interestingly, Ts65Dn femurs exhibited significantly lower toughness at 6 weeks of age, but by 16 weeks of age the difference no longer existed (Table 2). These data suggest that when geometry of the bone is considered, deficiencies in the structural and mineral composition of the Ts65Dn femur may not affect the overall strength of the bone.

Discussion

The present study revealed that Ts65Dn mice have lower trabecular bone volume and trabecular number and higher trabecular separation in the distal femur when compared to

euploid littermates. These results indicate that in addition to the trabeculae of craniofacial bones [29], the trabecular structure of the distal femur is affected in the Ts65Dn mouse. Along with the deficiencies observed in trabecular bone, cortical bone analysis showed a reduction in size of the midshaft and a smaller MPMI in the Ts65Dn femur. In addition to the structural findings in the Ts65Dn femur, BMD and BMC were significantly lower in the Ts65Dn femur indicating alterations in the mineral properties of the bone. Histomorphometric analysis revealed that the mineralizing surface on the periosteal bone surface was similar between Ts65Dn and euploid femurs. In contrast, MAR and BFR (DFR in incisor) were significantly lower in the femur and incisor of 6 week old Ts65Dn femurs. These results suggest that the bone deficiencies observed in the Ts65Dn femur and incisor are partly due to a reduction in osteoblast and odontoblast activity and not likely a reduction in cell number. Further analysis needs to be conducted to gain a better understanding of the affects of trisomy on osteoblasts and possibly osteoclasts in the Ts65Dn femur.

The changes observed in the physical structure and chemical properties of the Ts65Dn femur strongly suggested that the structural integrity of the bone was compromised as a result of trisomy. Three-point mechanical testing revealed a significantly lower ultimate load and stiffness, and thus compromised bone strength in the Ts65Dn femur. Furthermore, the material properties, obtained by normalizing the structural parameters with bone geometry, showed that the ultimate stress and modulus were not different between the two groups. However, toughness of the bone was significantly lower at 6 weeks of age in the Ts65Dn femur. The toughness of bone is directly related to the amount of collagen and how it is cross-linked in the extracellular matrix [30]. Our results suggest it is possible that Ts65Dn mice exhibit some form of collagen deficiency contributing to the Ts65Dn appendicular skeletal phenotype [31].

Densitometry analysis of the skull and femur of Ts65Dn mice show deficits in bone area, BMC, and BMD when compared to euploid littermates. A comparison of the percentage differences between 6 week Ts65Dn and euploid animals in femur and skull suggested that BMC and BMD of the trisomic femur were more affected than in the trisomic skull (32% vs. 15%; 22% vs. 5%, respectively) at this age, while the decreases in bone area were similar (9% vs. 10%). Interestingly, the femur is formed entirely via endochondral ossification where as only portions of the skull are formed from this process. It is plausible that Ts65Dn mice may exhibit a deficiency in endochondral ossification during skeletal development leading to the differences observed between the femur and the skull.

Comparison of the differences in several parameters between 6 and 16 week old trisomic bone further implicated the early stages of bone development as the possible origin to the Ts65Dn bone phenotype. Differences in BMC and BMD appeared greater between trisomic and euploid femur at 6 weeks of age compared to 16 weeks of age (32% vs. 21%; 22% vs. 8%, respectively), whereas these differences were similar in the skull across the two time points (5% vs. 7%; 15% vs. 14%). Further analysis of the structural properties of the femur also revealed that the percent differences observed in the femur were greater at 6 compared to 16 weeks of age for both trabecular (BV/TV, 43% vs. 25%; trabecular number, 39% vs. 22%; trabecular separation, 140% vs. 117%,) and cortical bone (area, 20% vs. 12%; perimeter, 11% vs. 6%; MPMI, 39% vs. 19%). Overall, these results suggest that the Ts65Dn appendicular skeletal phenotype may originate during critical stages of bone development and growth and persist through skeletal maturation leading to disruptions in bone homeostasis.

The Ts65Dn bone phenotype may also be influenced by factors other than age and trisomy. Differences in level of activity betweenTs65Dn and euploid mice could lead to the smaller, weaker bones observed. Yet, Ts65Dn mice have been shown to be more active than euploid

littermates [32,33], suggesting that activity levels are not contributing to the bone phenotypes observed in Ts65Dn mice. The consequences of this hyperactivity, however, may contribute to the smaller differences in the homeostatic measurements in 16 week old mice.

In addition to the data obtained on the femur, densitometry analysis showed reduction in BMD and BMC in the skull of Ts65Dn mice. Furthermore, analysis of the mineralization rate in the incisor showed that mineral apposition was significantly reduced in Ts65Dn mice. The skull and incisor are structures partially derived from neural crest cells [34,35], whereas the femur is derived from lateral plate mesoderm. It has been postulated that many of the craniofacial skeletal phenotypes associated with DS are neural crest derived [6,36] Comparison of mineralization data from the non-neural crest derived osteoblasts of the femur and the neural crest derived odontoblasts of the incisor show that mineralization is similarly affected in both tissues. These results suggest that in addition to cranial neural crest deficiencies, other mechanisms may be contributing to the Ts65Dn craniofacial phenotypes.

Ts65Dn mice have a smaller mandible at birth [21], and the origin of this defect begins as early in development as embryonic (E) day 9.25 [36]. Less is known regarding the origin of the appendicular skeletal defects presented in this study, but it is possible that reductions in mandible and femur size and composition are occurring via similar mechanisms as a result of trisomy. *Dyrk1a* and *Dscr1* are found in three copies in humans with DS as well as in the Ts65Dn mouse model [15,37]. It has been shown that these genes play a critical role in the regulation of Nuclear factor of activated t-cells (Nfat) activation via their distinct effects on the Calcineurin-Nfat pathway [38]. Recently it has been suggested that *Dyrk1a* regulates bone development and homeostasis (both bone formation and bone resorption) via negative feedback inhibition of Nfatc1 [39]. Based on this evidence, the theoretical overexpression of *Dyrk1a* and *Dscr1* in humans with DS and the Ts65Dn mouse model beginning in early development may disrupt normal bone homeostasis through the abnormal regulation of *Nfatc1*.

The disruption of normal bone development and homeostasis observed in the Ts65Dn mouse model may help uncover how trisomy affects skeletal development and growth as well as improving the quality of life for individuals with DS. Over the past century, average life span for individuals with DS has risen from 9 years in 1900 to over 50 years in 2000 [40], increasing the risk for ageing-related diseases such as osteoporosis. In addition to an increased life expectancy, individuals with DS exhibit reductions in BMD associated with hypotonia, as well as nutritional and hormone deficiencies [41], suggesting that these individuals may be more susceptible to osteoporosis. A study conducted on a small population of women with DS found that women with DS have an increased rate of osteoporosis compared to normal individuals [42]. The possibility for increased incidence of osteoporosis in individuals with DS adds to our need to better understand DS bone phenotypes.

Based on our findings in the Ts65Dn mouse model, the trismic appendicular skeleton is severely affected at a young age and this affect continues through development to adulthood. Specifically, trabecular bone is less abundant and poorly connected similar to what is observed in osteoporosis. Also, bone formation is slower and the mechanical properties of the bone are weakened. The greater differences observed in trabecular and cortical bone structure, BMC, BMD, and bone area in trisomic compared to euploid femurs at 6 weeks of age when compared to 16 weeks of age, suggest it is likely that deficiencies in the Ts65Dn appendicular skeleton originate during the early stages of bone development and growth and continue through maturation. Overall, these results suggest that individuals with DS may have an increased risk for developmental bone abnormalities, compromised bone strength,

and/or early onset osteoporosis due to a likely combination of altered developmental and homeostatic bone mechanisms.

Further studies are needed to elucidate the underlying molecular and cellular mechanisms contributing to the altered bone phenotypes and identify the developmental and/or homeostatic origin of these phenotypes observed in the Ts65Dn mouse model. Uncovering the specific contributions of osteoblasts and osteoclasts to the trisomic bone phenotypes as well as analysis of embryonic and early postnatal cartilage templates may prove to be crucial steps in developing prevention and treatment therapies with the hopes of improving the quality of life for individuals with DS.

Acknowledgments

We are grateful to Jared Allen for his help with Image J analysis, Tyler Nelson for assistance with the three-point bending protocol, Dr. Keith Condon for his expertise in bone histology and sectioning, and Dr. Matt Allen for his assistance with MicroCT training and data analysis. This work was supported by an Honors Program Research Fellowship (Randall J. Roper and Anna Gaddy), Undergraduate Research Opportunity Grants (Anna Gaddy and Rachel Meyer) from IUPUI, an NSF GK-12 fellowship (Joshua D. Blazek), a gift from the Beaty/C-Tech fund--Blue River Community Foundations (Randall J. Roper) and a MicroCT equipment grant from the NIH (S10-RR023710).

References

1. Schieve LA, Boulet SL, Boyle C, Rasmussen SA, Schendel D. Health of children 3 to 17 years of age with Down syndrome in the 1997-2005 national health interview survey. Pediatrics 2009;123:e253–60. [PubMed: 19171577]
2. Cleves MA, Hobbs CA, Cleves PA, Tilford JM, Bird TM, Robbins JM. Congenital defects among liveborn infants with Down syndrome. Birth Defects Res A Clin Mol Teratol 2007;79:657–63. [PubMed: 17696161]
3. Richtsmeier JT, Zumwalt A, Carlson EJ, Epstein CJ, Reeves RH. Craniofacial phenotypes in segmentally trisomic mouse models for Down syndrome. Am J Med Genet 2002;107:317–24. [PubMed: 11840489]
4. Van Cleve SN, Cohen WI. Part I: clinical practice guidelines for children with Down syndrome from birth to 12 years. J Pediatr Health Care 2006;20:47–54. [PubMed: 16399479]
5. Van Cleve SN, Cannon S, Cohen WI. Part II: Clinical Practice Guidelines for adolescents and young adults with Down Syndrome: 12 to 21 Years. J Pediatr Health Care 2006;20:198–205. [PubMed: 16675381]
6. Richtsmeier JT, Baxter LL, Reeves RH. Parallels of craniofacial maldevelopment in Down syndrome and Ts65Dn mice. Dev Dyn 2000;217:137–45. [PubMed: 10706138]
7. Alio JJ, Lorenzo J, Iglesias C. Cranial base growth in patients with Down syndrome: a longitudinal study. Am J Orthod Dentofacial Orthop 2008;133:729–37. [PubMed: 18456147]
8. de Moraes ME, Tanaka JL, de Moraes LC, Filho EM, de Melo Castilho JC. Skeletal age of individuals with Down syndrome. Spec Care Dentist 2008;28:101–6. [PubMed: 18489657]
9. Keeling JW, Hansen BF, Kjaer I. Pattern of malformations in the axial skeleton in human trisomy 21 fetuses. Am J Med Genet 1997;68:466–71. [PubMed: 9021023]
10. Longo D, DeFigueiredo D, Cicero S, Sacchini C, Nicolaides KH. Femur and humerus length in trisomy 21 fetuses at 11-14 weeks of gestation. Ultrasound Obstet Gynecol 2004;23:143–7. [PubMed: 14770393]
11. Gray DL, Dicke JM, Dickerson R, McCourt C, Odibo AO. Reevaluating humeral length for the detection of fetal trisomy 21. J Ultrasound Med 2009;28:1325–30. [PubMed: 19778878]
12. Weisz B, David AL, Chitty L, Peebles D, Pandya P, Patel P, Rodeck CH. Association of isolated short femur in the mid-trimester fetus with perinatal outcome. Ultrasound Obstet Gynecol 2008;31:512–6. [PubMed: 18432603]
13. Guijarro M, Valero C, Paule B, Gonzalez-Macias J, Riancho JA. Bone mass in young adults with Down syndrome. J Intellect Disabil Res 2008;52:182–9. [PubMed: 18261017]

14. Baptista F, Varela A, Sardinha LB. Bone mineral mass in males and females with and without Down syndrome. Osteoporos Int 2005;16:380–8. [PubMed: 15365695]
15. Reeves RH, Irving NG, Moran TH, Wohn A, Kitt C, Sisodia SS, Schmidt C, Bronson RT, Davisson MT. A mouse model for Down syndrome exhibits learning and behaviour deficits. Nat Genet 1995;11:177–84. [PubMed: 7550346]
16. Hattori M, Fujiyama A, Sakaki Y. The DNA sequence of human chromosome 21. Tanpakushitsu Kakusan Koso 2001;46:2254–61. [PubMed: 11802376]
17. Gardiner K, Fortna A, Bechtel L, Davisson MT. Mouse models of Down syndrome: how useful can they be? Comparison of the gene content of human chromosome 21 with orthologous mouse genomic regions. Gene 2003;318:137–47. [PubMed: 14585506]
18. Holtzman DM, Santucci D, Kilbridge J, Chua-Couzens J, Fontana DJ, Daniels SE, Johnson RM, Chen K, Sun Y, Carlson E, Alleva E, Epstein CJ, Mobley WC. Developmental abnormalities and age-related neurodegeneration in a mouse model of Down syndrome. Proc Natl Acad Sci U S A 1996;93:13333–8. [PubMed: 8917591]
19. Moore CS, Roper RJ. The power of comparative and developmental studies for mouse models of Down syndrome. Mamm Genome 2007;18:431–43. [PubMed: 17653795]
20. Wiseman FK, Alford KA, Tybulewicz VL, Fisher EM. Down syndrome--recent progress and future prospects. Hum Mol Genet 2009;18:R75–83. [PubMed: 19297404]
21. Hill CA, Reeves RH, Richtsmeier JT. Effects of aneuploidy on skull growth in a mouse model of Down syndrome. J Anat 2007;210:394–405. [PubMed: 17428201]
22. Baxter LL, Moran TH, Richtsmeier JT, Troncoso J, Reeves RH. Discovery and genetic localization of Down syndrome cerebellar phenotypes using the Ts65Dn mouse. Hum Mol Genet 2000;9:195–202. [PubMed: 10607830]
23. Li J, Meyer R, Duncan RL, Turner CH. P2X7 nucleotide receptor plays an important role in callus remodeling during fracture repair. Calcif Tissue Int 2009;84:405–12. [PubMed: 19308630]
24. McCarthy EA, Raggio CL, Hossack MD, Miller EA, Jain S, Boskey AL, Camacho NP. Alendronate treatment for infants with osteogenesis imperfecta: demonstration of efficacy in a mouse model. Pediatr Res 2002;52:660–70. [PubMed: 12409511]
25. Turner CH, Burr DB. Basic biomechanical measurements of bone: a tutorial. Bone 1993;14:595–608. [PubMed: 8274302]
26. Allen MR, Reinwald S, Burr DB. Alendronate reduces bone toughness of ribs without significantly increasing microdamage accumulation in dogs following 3 years of daily treatment. Calcif Tissue Int 2008;82:354–60. [PubMed: 18463913]
27. Kohler T, Beyeler M, Webster D, Muller R. Compartmental bone morphometry in the mouse femur: reproducibility and resolution dependence of microtomographic measurements. Calcif Tissue Int 2005;77:281–90. [PubMed: 16283571]
28. Masinde GL, Li X, Gu W, Wergedal J, Mohan S, Baylink DJ. Quantitative trait loci for bone density in mice: the genes determining total skeletal density and femur density show little overlap in F2 mice. Calcif Tissue Int 2002;71:421–8. [PubMed: 12202954]
29. Parsons T, Ryan TM, Reeves RH, Richtsmeier JT. Microstructure of trabecular bone in a mouse model for Down syndrome. Anat Rec (Hoboken) 2007;290:414–21. [PubMed: 17514765]
30. Burr DB. Bone material properties and mineral matrix contributions to fracture risk or age in women and men. J Musculoskelet Neuronal Interact 2002;2:201–4. [PubMed: 15758433]
31. Viguet-Carrin S, Garnero P, Delmas PD. The role of collagen in bone strength. Osteoporos Int 2006;17:319–36. [PubMed: 16341622]
32. Stewart LS, Persinger MA, Cortez MA, Snead OC 3rd. Chronobiometry of behavioral activity in the Ts65Dn model of Down syndrome. Behav Genet 2007;37:388–98. [PubMed: 17146725]
33. Escorihuela RM, Fernandez-Teruel A, Vallina IF, Baamonde C, Lumbreras MA, Dierssen M, Tobena A, Florez J. A behavioral assessment of Ts65Dn mice: a putative Down syndrome model. Neurosci Lett 1995;199:143–6. [PubMed: 8584244]
34. Mitsiadis TA, Graf D. Cell fate determination during tooth development and regeneration. Birth Defects Res C Embryo Today 2009;87:199–211. [PubMed: 19750524]

35. Gitton Y, Heude E, Vieux-Rochas M, Benouaiche L, Fontaine A, Sato T, Kurihara Y, Kurihara H, Couly G, Levi G. Evolving maps in craniofacial development. Semin Cell Dev Biol 2010;21:301–8. [PubMed: 20083217]
36. Roper RJ, VanHorn JF, Cain CC, Reeves RH. A neural crest deficit in Down syndrome mice is associated with deficient mitotic response to Sonic hedgehog. Mech Dev 2009;126:212–9. [PubMed: 19056491]
37. Gitton Y, Dahmane N, Baik S, Ruiz i Altaba A, Neidhardt L, Scholze M, Herrmann BG, Kahlem P, Benkahla A, Schrinner S, Yildirimman R, Herwig R, Lehrach H, Yaspo ML. A gene expression map of human chromosome 21 orthologues in the mouse. Nature 2002;420:586–90. [PubMed: 12466855]
38. Arron JR, Winslow MM, Polleri A, Chang CP, Wu H, Gao X, Neilson JR, Chen L, Heit JJ, Kim SK, Yamasaki N, Miyakawa T, Francke U, Graef IA, Crabtree GR. NFAT dysregulation by increased dosage of DSCR1 and DYRK1A on chromosome 21. Nature 2006;441:595–600. [PubMed: 16554754]
39. Lee Y, Ha J, Kim HJ, Kim YS, Chang EJ, Song WJ, Kim HH. Negative feedback Inhibition of NFATc1 by DYRK1A regulates bone homeostasis. J Biol Chem 2009;284:33343–51. [PubMed: 19801542]
40. Brown R, Taylor J, Matthews B. Quality of life--ageing and Down syndrome. Downs Syndr Res Pract 2001;6:111–6. [PubMed: 11501212]
41. Hawli Y, Nasrallah M, El-Hajj Fuleihan G. Endocrine and musculoskeletal abnormalities in patients with Down syndrome. Nat Rev Endocrinol 2009;5:327–34. [PubMed: 19421241]
42. Center J, Beange H, McElduff A. People with mental retardation have an increased prevalence of osteoporosis: a population study. Am J Ment Retard 1998;103:19–28. [PubMed: 9678227]
43. Moore CS, Lee JS, Birren B, Stetten G, Baxter LL, Reeves RH. Integration of cytogenetic with recombinational and physical maps of mouse chromosome 16. Genomics 1999;59:1–5. [PubMed: 10395793]

Abbreviations: The abbreviations used are

DS	Down syndrome
MPMI	mean polar moment of inertia
BMD	bone mineral density
BMC	bone mineral content
DXA	Dual energy x-ray absorptiometry
Ts	trisomic
Eu	euploid
BFR	bone formation rate
DFR	dentin formation rate
MAR	mineral apposition rate

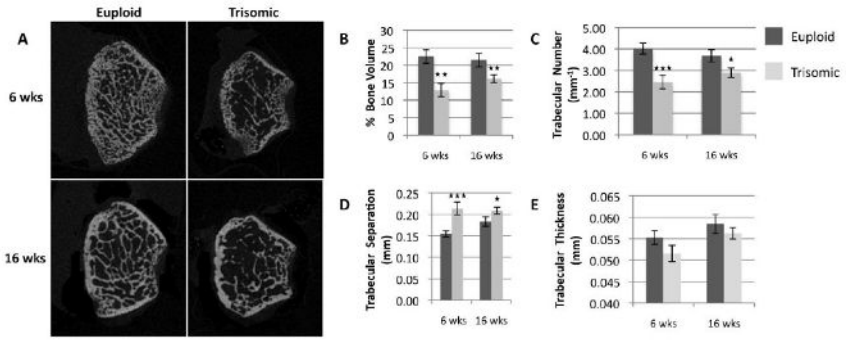

Figure 1. MicroCT analysis of trabecular bone in the Ts65Dn femur

MicroCT images of the distal femur in euploid and trisomic mice at the ages of 6 and 16 weeks (A). Analysis revealed a significant reduction in percent bone volume (B) and number of trabeculae (C), as well as a significant increase in trabecular separation (D) at both time points in trisomic mice. Although smaller, no significant difference was found in trabecular thickness (E) between the two groups. (Eu 6 wks, n= 12; Ts 6 wks, n= 10; Eu 16 wks, n= 10; Ts 16 wks, n= 16) (*$p \leq 0.05$, **$p \leq 0.01$, *** $p \leq 0.001$)

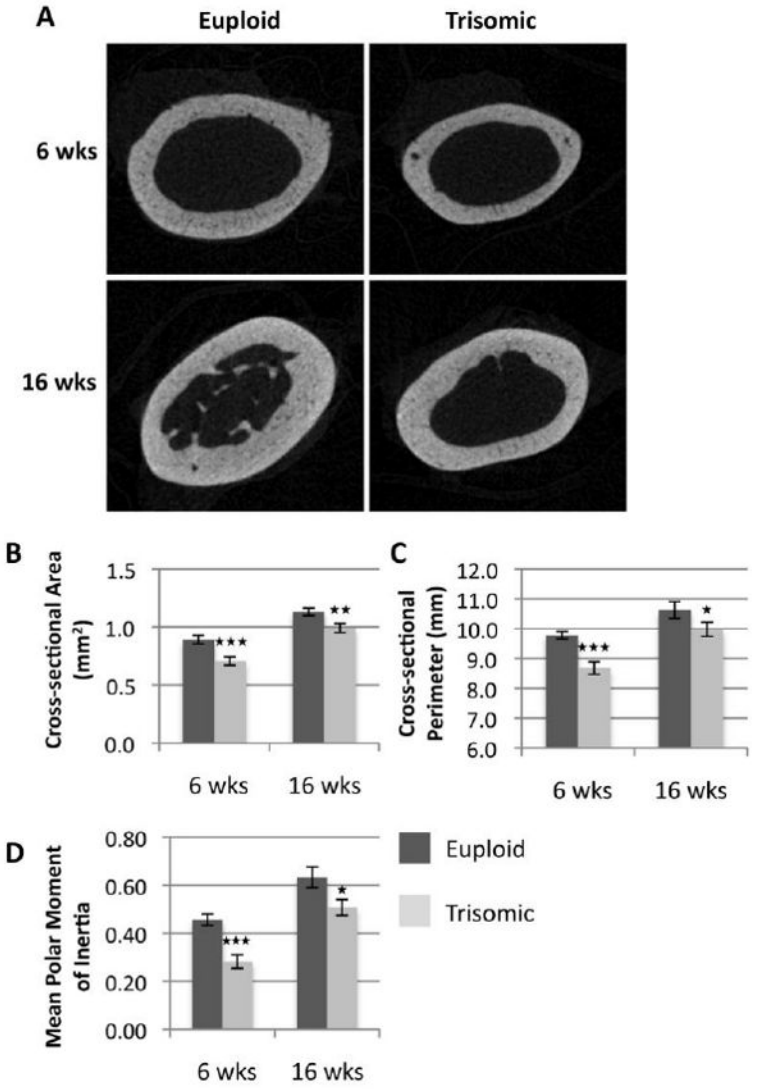

Figure 2. MicroCT analysis of cortical bone in the Ts65Dn femur

MicroCT images of the femur midshaft in euploid and trisomic mice at the ages of 6 and 16 weeks (A). Analysis revealed significant reductions in MPMI (B), cross-sectional bone area (C), and periosteal bone perimeter (D). (Eu 6 wks, n= 12; Ts 6 wks, n= 10; Eu 16 wks, n= 10; Ts 16 wks, n= 15) (*$p \leq 0.05$, **$p \leq 0.01$, *** $p \leq 0.001$)

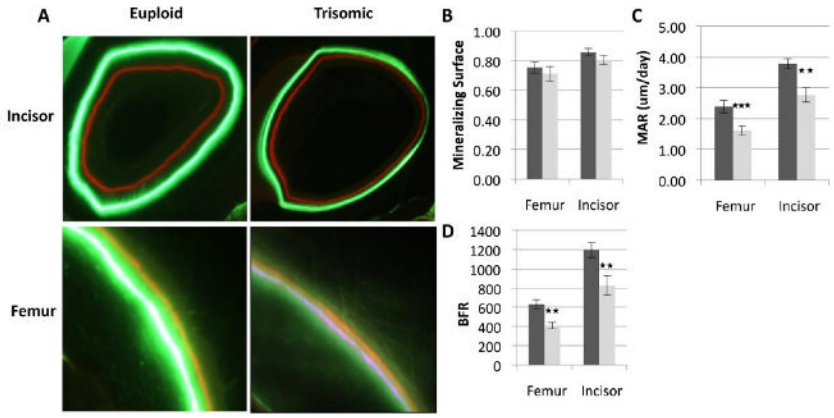

Figure 3. Dynamic bone formation properties in the Ts65Dn incisor and femur

Fluorescent labeling using Calcein green and Alizarin red staining in the incisor and femur of euploid and trisomic mice, respectively, at the age of 6 weeks (A). Mineralizing surface (B) was not significantly different in the femur or incisor between Ts65Dn and euploid mice. Mineral apposition rate (C) and bone formation rate (D) was significantly reduced in Ts65Dn mice in both the incisor and the femur. (Incisor; Eu, n= 13; Ts, n= 10; Femur; Eu, n= 11; Ts, n= 8)(**$p \leq 0.01$, *** $p \leq 0.001$)

Table 1
Densitometry analysis reveals altered bone composition in Ts65Dn mice

	6 Weeks of Age		16 Weeks of Age	
	Euploid	**Trisomic**	**Euploid**	**Trisomic**
Femur	n=18	n=16	n=17	n=22
Area (cm^2)	0.411 (0.015)	0.374 (0.013)*	0.536 (0.012)	0.458 (0.010)***
BMD (g/cm^2)	0.059 (0.002)	0.046 (0.001)***	0.071 (0.001)	0.065 (0.002)*
BMC (g)	0.025 (0.001)	0.017 (0.001)***	0.038 (0.001)	0.030 (0.001)***
Skull	n=7	n=16	n=10	n=9
Area (cm^2)	2.241 (0.038)	2.008 (0.025)***	2.475 (0.034)	2.281 (0.032)***
BMD (g/cm^2)	0.099 (0.002)	0.094 (0.002)*	0.118 (0.002)	0.110 (0.003)**
BMC (g)	0.222 (0.007)	0.188 (0.004)***	0.292 (0.004)	0.252 (0.008)***

Data are presented mean ± (SEM).

* $p \leq 0.05$

** $p \leq 0.01$

*** $p \leq 0.001$

Table 2
Mechanical properties of the Femur at 6 and 16 weeks of age

	Eu 6 Weeks n=3	Ts 6 Weeks n=13	Eu 16 Weeks n=5	Ts16 Weeks n=12
Ultimate Load (N)	22.51 (3.70)	16.36 (1.21)*	24.98 (1.29)	21.47 (0.88)*
Energy to Failure (mJ)	5.72 (1.23)	4.08 (0.31)*	11.86 (0.53)	10.24 (0.60)
Stiffness (N/mm)	11.15 (2.66)	6.91 (0.63)*	29.67 (2.34)	24.40 (0.89)**
CSMI (mm^4)	0.105 (0.009)	0.066 (0.004)**	0.152 (0.019)	0.092 (0.006)**
Ultimate Stress (N/mm^2)	265.33 (59.01)	231.71 (6.33)	240.45 (21.73)	294.26 (15.92)
Young's Modulus (N/mm^2)	1037.54 (369.18)	1055.92 (69.54)	2293.31 (445.84)	2934.35 (191.44)
Toughness (mJ/m^3)	10.27 (2.77)	6.52 (0.50)*	14.71 (0.87)	16.02 (0.91)

Data are presented mean ± (SEM).

* $p \leq 0.05$

** $p \leq 0.01$